

# Hydrophobic and Hydrophilic Balance and Its Effect on Mesophase Behaviour in Hydroxyalkyl Ethers of Methyl Glucopyranoside

Madan K. Singh,<sup>[a, c]</sup> Rui Xu,<sup>[a, c]</sup> Sylvie Moebs,<sup>[a, c]</sup> Anil Kumar,<sup>[d]</sup> Yves Queneau,<sup>\*,[a, c]</sup> Stephen J. Cowling,<sup>\*,[b]</sup> and John W. Goodby<sup>[b]</sup>

**Abstract:** Four series of monosubstituted methyl  $\alpha$ -D-glucopyranoside hydroxyalkyl ethers were prepared and their thermotropic and lyotropic self-organising properties were investigated in terms of the hydrophobic–hydrophilic balance with respect to their molecular structures. The results obtained lead us to a new understanding of the forces that drive the formation of condensed soft-matter phases.

**Keywords:** carbohydrates • liquid crystals • mesophases • self-assembly • soft matter

## Introduction

Liquid crystals are classically split into two forms: lyotropic and thermotropic. The two appear to be separate; lyotropic phases are composed of an amphiphile and an appropriate liquid over a defined concentration range, whereas thermotropic phases are usually based on single-component systems that form condensed phases as a function of temperature. Lyotropic and thermotropic liquid crystals exhibit polymorphism as a function of concentration and temperature, respectively. Amphitropic liquid crystals are materials that can exhibit both types of phases. Glycolipids can be amphitropic and exhibit the full range of lyotropic phases as a function of concentration in water, but they essentially exhibit one thermotropic phase (i.e., the lamellar/smectic A phase).<sup>[1]</sup> In the case of both types, a balance exists with respect to the molecular architectures of the components (e.g., flexible/rigid, polar/non-polar, hydrogen-bonding/non-hydrogen-bonding, aromatic/aliphatic and so on). Thermotropic liquid crystals are very sensitive to the various intra-molecular bal-

ances as witnessed by the development of materials for applications in displays. Conversely, lyotropic liquid crystals are less sensitive, and are primarily affected by the polar/non-polar balance and the curvature of packing of the amphiphiles in the solvent, which is a manifestation of the “hydrophobic effect”.<sup>[2]</sup>

The type of lyotropic phase formed by an amphiphile can often be predicted by using the dimensionless packing parameter  $S$ . This simple model takes into account free energies of interaction, molecular geometry and entropy. Thus it is useful in determining the size and shape of amphiphilic aggregates.  $S$  is given by  $S = V/al$ , in which  $V$  is the hydrocarbon volume,  $a$  is the area of the head group and  $l$  is the critical length of the hydrocarbon chain.<sup>[3–6]</sup> The value of  $S$  determines the aggregate formed by amphiphiles upon hydration. It has been shown that spherical micelles are formed for  $S < 1/3$ , hexagonal phases for  $1/3 < S < 1/2$ , lamellar for  $1/2 < S < 1$  and reverse micelles or hexagonal phases for  $S > 1$ . However, caution has to be taken when using this model because the limits set on the values of  $S$  predicted above are relatively insensitive to the exact values of  $V$  and  $a$  but are strongly dependent upon the choice of  $l$ .<sup>[7–9]</sup> For thermotropic systems, phase formation is not so predictive because the inter-molecular interactions are usually weaker and there are a number of structural balances in play at the same time, as illustrated in some of our previous studies that involve sucrose-based compounds.<sup>[10–12]</sup> However, one family of substituted sugar-based polyols has been shown to exhibit predictive properties. Figure 1 shows the transition temperatures for the clearing points of dodecyl-substituted acyclic polyols, which increase linearly with the number of hydroxyl groups.<sup>[1,13]</sup> In addition, it was also found that there was little or no effect of molecular chirality on the clearing points. Thus, for this family of compounds there is one dominant effect and that is the hydrophobic–hydrophilic balance, which is typical of lyotropic systems.

In the present study, we have examined the role of the hydrophobic–hydrophilic balance on the self-organising properties of the monosubstituted methyl  $\alpha$ -D-glucopyranoside

[a] Dr. M. K. Singh, R. Xu, Dr. S. Moebs, Dr. Y. Queneau  
INSA Lyon, ICBMS, Bâtiment J. Verne  
20 av A. Einstein, 69621 Villeurbanne (France)  
E-mail: yves.queneau@insa-lyon.fr

[b] Dr. S. J. Cowling, Prof. J. W. Goodby  
Department of Chemistry, The University of York  
York, YO10 5DD (UK)  
E-mail: Stephen.cowling@york.ac.uk

[c] Dr. M. K. Singh, R. Xu, Dr. S. Moebs, Dr. Y. Queneau  
CNRS, UMR 5246, ICBMS, Université Lyon 1  
INSA-Lyon; CPE-Lyon, Bâtiment CPE  
43 bd du 11 novembre 1918  
69622 Villeurbanne (France)

[d] Dr. A. Kumar  
Physical and Materials Chemistry Division  
National Chemical Laboratory  
Pune - 411008 (India)

Supporting information for this article is available on the WWW under <http://dx.doi.org/10.1002/chem.201202933>.

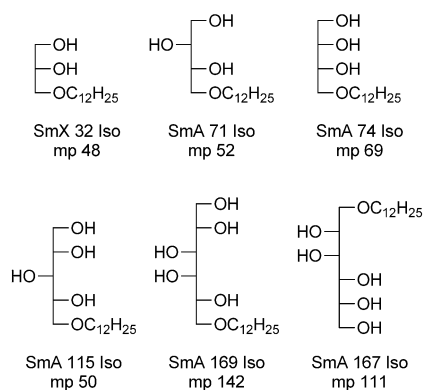


Figure 1. Effect of the number of hydroxyl groups on clearing-point and melting temperatures.<sup>[1]</sup>

hydroxyalkyl ethers, and we have developed a new concept for the formation and stabilisation of thermotropic liquid-crystal phases. The structure of the materials used in this study is summarised in Figure 2.



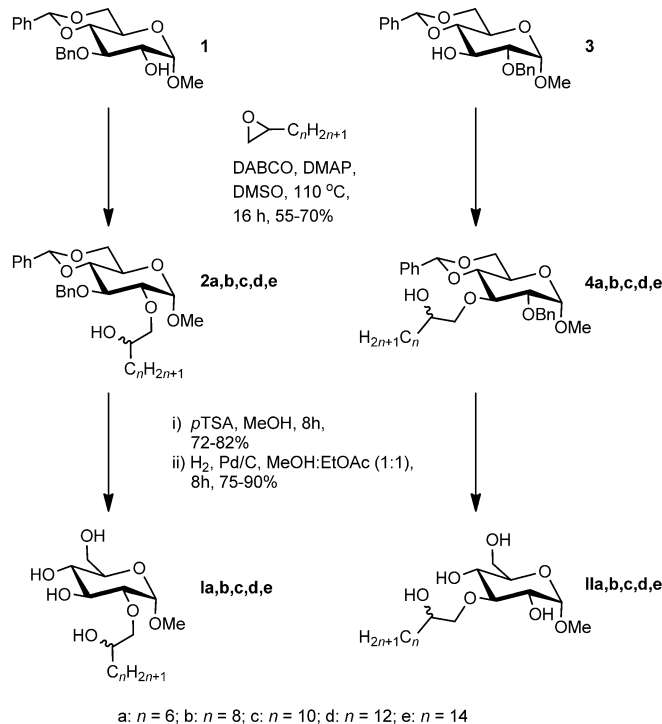
Figure 2. Substitution positions around the glucose unit (left) and the hydroxyalkyl chain (right) of the compounds examined in this study.

## Results and Discussion

**Synthesis:** The general methods, syntheses and analytical data for all of the compounds in this article are given in the Supporting Information.

All hydroxyalkyl ethers were obtained by unambiguous routes from the corresponding partially protected methyl glucosides, which have only one available OH group ready for etherification. For methyl 2-*O*-(2-hydroxyalkyl)- $\alpha$ -D-glucopyranosides (**I**) and methyl 3-*O*-(2-hydroxyalkyl)- $\alpha$ -D-glucopyranosides (**II**), the synthesis started from monobenzylated methyl 4,6-*O*-benzylidene- $\alpha$ -D-glucopyranoside **1** and **3**,<sup>[14]</sup> which can be obtained from methyl 4,6-*O*-benzylidene- $\alpha$ -D-glucopyranoside and benzyl bromide in the presence of tetrabutylammonium iodide. This can be achieved by two methods, either by means of the intermediate stannylene formed by reaction with dibutyltin oxide<sup>[15]</sup> or under heterogeneous conditions using aqueous NaOH in dichloromethane at room temperature.<sup>[16]</sup> Both methods give mixtures of the two possible monobenzylated products at *O*-2 or at *O*-3 in slightly different ratio. Reaction of 1,2-epoxyalkanes with methyl 2- or 3-*O*-benzyl-4,6-*O*-benzylidene- $\alpha$ -D-glucopyranosides was performed in dimethylsulfoxide (DMSO) in the presence of 1,4-diazabicyclo[2.2.2]octane (DABCO) and dimethylaminopyridine (DMAP) as basic catalysts on the basis of our previous studies for epoxide opening by sugars.<sup>[17-20]</sup> The reaction yielded methyl 3-*O*-benzyl-2-*O*-(2-

hydroxyalkyl)-4,6-*O*-benzylidene- $\alpha$ -D-glucopyranosides (**2**) or 2-*O*-benzyl-3-*O*-(2-hydroxyalkyl)-4,6-*O*-benzylidene- $\alpha$ -D-glucopyranosides (**4**) in 55–70% yield. Deprotection by acidic treatment (catalyst: *p*-toluenesulfonic acid in methanol) followed by Pd-catalysed hydrogenation in MeOH/EtOAc afforded methyl 2-*O*-(2-hydroxyalkyl)- $\alpha$ -D-glucopyranosides (**I**) and 3-*O*-(2-hydroxyalkyl)- $\alpha$ -D-glucopyranosides (**II**; see Scheme 1). The final hydroxyalkyl ethers are

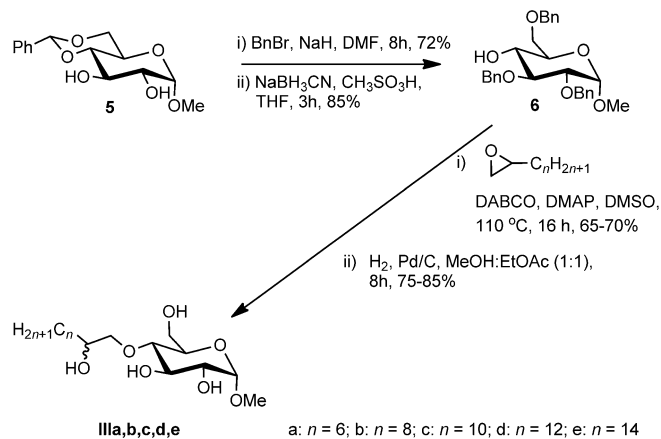


Scheme 1. Synthesis of methyl 2-*O*-(2-hydroxyalkyl)- $\alpha$ -D-glucopyranosides (**I**) and 3-*O*-(2-hydroxyalkyl)- $\alpha$ -D-glucopyranosides (**II**).

actually mixtures of two diastereoisomers that are epimers at the CHOH group newly formed by the opening of the epoxide. The <sup>13</sup>C NMR spectroscopic analysis reveals a very slight differentiation in chemical shifts for both isomers of this CHOH and some of the carbon atoms of the neighbouring CH<sub>2</sub> groups. In crude mixtures, a 1:1 mixture of both isomers has been observed (within the limits of <sup>13</sup>C NMR spectroscopy), which means that no diastereomeric discrimination occurred at the epoxide ring-opening reaction. Both isomers might, however, differ slightly in their behaviour during the purification steps by silica gel chromatography, therefore it was carefully verified at the final purification step of the materials that all of the samples used in our studies were consistent 1:1 mixtures.

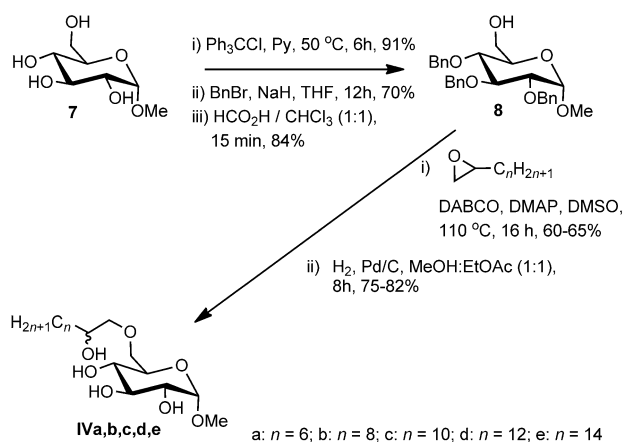
To obtain methyl 4-*O*-(2-hydroxyalkyl)- $\alpha$ -D-glucopyranosides (**III**), methyl 4,6-*O*-benzylidene- $\alpha$ -D-glucopyranoside (**5**) was treated with benzyl bromide in the presence of NaH/DMF followed by selective reductive opening of the benzylidene ring with NaBH<sub>3</sub>CN/CH<sub>3</sub>SO<sub>3</sub>H/THF to give methyl 2,3,6-tri-*O*-benzyl- $\alpha$ -D-glucopyranoside (**6**).<sup>[21]</sup> Com-

compound **6** was treated with 1,2-epoxyalkanes in DMSO in the presence of DABCO/DMAP to yield benzylated 4-*O*-(2-hydroxyalkyl) ethers of methyl glucoside, which was deprotected by Pd-catalysed hydrogenation in MeOH/EtOAc to afford methyl 4-*O*-(2-hydroxyalkyl)- $\alpha$ -D-glucopyranosides **III** (see Scheme 2)



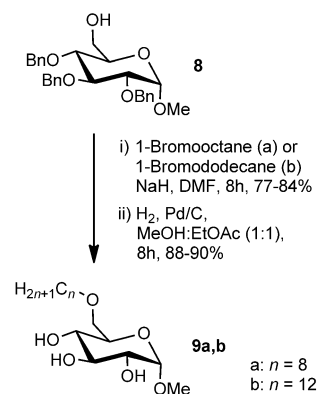
Scheme 2. Synthesis of methyl 4-*O*-(2-hydroxyalkyl)- $\alpha$ -D-glucopyranosides (**III**).

For the 6-substituted hydroxyalkyl ethers (**IV**), the sequence started with the tritylation and subsequent benzylation of methyl  $\alpha$ -D-glucopyranoside, which afforded methyl 2,3,4-tri-*O*-benzyl-6-*O*-trityl- $\alpha$ -D-glucopyranoside. This was deprotected under acidic conditions to give compound **8**, in which only OH-6 was available. The structure of this compound was confirmed by comparison with an identical compound obtained from an alternative reductive opening of the benzylidene.<sup>[21]</sup> Compound **8** was reacted with 1,2-epoxyalkanes in DMSO in the presence of DABCO and DMAP at 110 °C for 16 h, followed by catalytic hydrogenation to give the desired methyl 6-*O*-(2-hydroxyalkyl)- $\alpha$ -D-glucopyranosides (**IV**; see Scheme 3).



Scheme 3. Synthesis of methyl 6-*O*-(2-hydroxyalkyl)- $\alpha$ -D-glucopyranosides (**IV**).

For the purpose of comparison, two non-branched 6-*O*-alkyl- $\alpha$ -D-glucopyranosides (**9**) were prepared by the reaction of methyl 2,3,4-tri-*O*-benzyl- $\alpha$ -D-glucopyranoside (**8**) with 1-bromooctane or 1-bromododecane in the presence of NaH/DMF to give methyl 2,3,4-tri-*O*-benzyl-6-*O*-alkyl- $\alpha$ -D-glucopyranoside, which was debenzylated by Pd-catalysed hydrogenation in MeOH/EtOAc (see Scheme 4).<sup>[22–24]</sup>



Scheme 4. Synthesis of 6-*O*-alkyl- $\alpha$ -D-glucopyranosides **9**.

**Thermotropic behaviour:** All of the compounds were examined by polarised light microscopy and differential scanning calorimetry (DSC). The specific methods for microscopy and differential scanning calorimetry are given in the Supporting Information. The results are given in Tables 1–5 in which the values given represent those observed upon heating the sample except for glass transitions, which are observed on cooling.

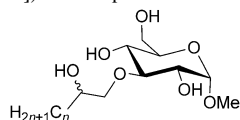
Table 1. Transition temperatures [°C] and enthalpy of transition (in square brackets [kJ mol<sup>-1</sup>]) for compounds **I**a–**e**.<sup>[a]</sup>

Compound	<i>n</i>	K	SmA	Iso	<i>T</i> <sub>g</sub>
<b>I</b> a	6	• 49.4 [41.08]	–	–	• –11.5
<b>I</b> b	8	• 33.0 [7.67]	–	–	• –11.5
<b>I</b> c	10	• 59.7 [33.03]	(• 39.8) [0.58]	•	• 8.2
<b>I</b> d	12	• 62.8 [29.11]	• 73.7 [0.72]	•	• –
<b>I</b> e	14	• 69.2/78.2 [23.76/13.53]	• 94.8 [0.96]	•	• –

[a] See Figure 2 for definition of *n*; K = crystal; SmA = smectic A; Iso = isotropic liquid; *T*<sub>g</sub> = glass-transition temperature. A • identifies that the phase is observed for the compound. Parentheses indicate that the phase is monotropic (i.e., occurring only on cooling below the melting point).

For the homologous series of compounds examined, the longer-chain homologues were found to exhibit thermotropic, lamellar (smectic A) phases, whereas the short-chain-length members did not possess mesomorphic properties. Those compounds, which did exhibit mesomorphism, behaved in a similar way; for the lower homologues, when the

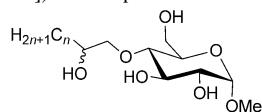
Table 2. Transition temperatures [°C] and enthalpy of transition (in square brackets [kJ mol<sup>-1</sup>]) for compounds **IIa–e**.



Compound	<i>n</i>	K	SmA	Iso	<i>T<sub>g</sub></i>
<b>IIa</b>	6	–	–	–	–5.4
<b>IIb</b>	8	• 8.1 [1.22]	–	–	–9.8
<b>IIc</b>	10	• –	• 48.7 <sup>[a]</sup> [1.27]	•	–6.6
<b>IId</b>	12	• 32.7 [13.95]	• 66.2 [2.17]	•	–
<b>IIe</b>	14	• 43.9 [31.29]	• 85.0 [1.02]	•	–

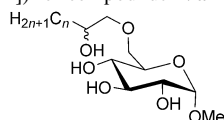
[a] There is a second peak at 42.0 °C.

Table 3. Transition temperatures [°C] and enthalpy of transition (in square brackets [kJ mol<sup>-1</sup>]) for compounds **IIIa–e**.



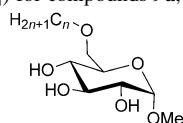
Compound	<i>n</i>	K	SmA	Iso	<i>T<sub>g</sub></i>
<b>IIIa</b>	6	• 25.2/31.3 [0.79/2.17]	–	–	–14.7
<b>IIIb</b>	8	• 64.2 [9.17]	–	–	–1.3
<b>IIIc</b>	10	• 33.7 [21.08]	–	–	–4.2
<b>IIId</b>	12	• 34.5 [21.56]	• 62.6 [0.11]	•	–
<b>IIIe</b>	14	• 39.7 [25.09]	• 81.3 [0.73]	•	–

Table 4. Transition temperatures [°C] and enthalpy of transition (in square brackets [kJ mol<sup>-1</sup>]) for compounds **IVa–IV**.



Compound	<i>n</i>	K	SmA	Iso	<i>T<sub>g</sub></i>
<b>IVa</b>	6	–	–	–	–
<b>IVb</b>	8	• 47.9 [19.43]	–	–	–2.1
<b>IVc</b>	10	• 64.8 [30.65]	(• 37.9) [0.74]	•	0.3
<b>IVd</b>	12	• 71.3 [33.96]	(• 58.5) [0.89]	•	–
<b>IVe</b>	14	• 72.8 [32.57]	• 79.0 [0.69]	•	–

Table 5. Transition temperatures [°C] and enthalpy of transition (in square brackets [kJ mol<sup>-1</sup>]) for compounds **9a,b**.



Compound	<i>n</i>	K	SmA	Iso	<i>T<sub>g</sub></i>
<b>9a</b>	8	–	• 20.1 [0.77]	•	–22.6
<b>9b</b>	12	• 56.5 [35.83]	(• 33.3) [0.90]	•	–

lamellar phase was observed, the materials tended to favour homeotropic orientation (i.e., in which the long axes of the molecules are oriented perpendicular to the plane of the microscope slide). This is probably due to the dominant interaction between the glass surface and the hydroxyl groups of the glucoside head group. These interactions dominate the

contributions of the aliphatic chains to the alignment. For the higher homologues (*n* = 12 and 14), the defect textures, seen through the use of transmission polarised light microscopy, exhibited focal-conic defects characterised by elliptical and hyperbolic lines of optical discontinuity, accompanied by regions of homeotropic alignment; see, for example, Figure 3 for compound **Ie**. This combination of defect textures is diagnostic for the smectic A phase.

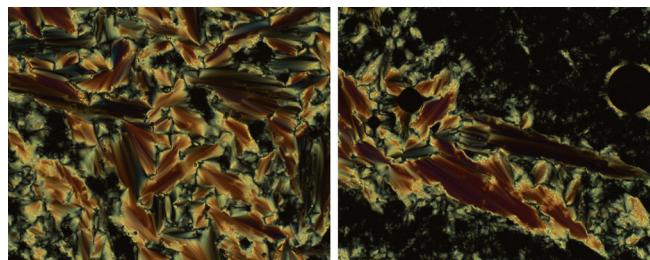


Figure 3. Photomicrographs (100× magnification) of the lamellar phase of compound **Ie** at 90 °C showing focal-conic and homeotropic domains.

Interestingly, the homologues of all four series with relatively short aliphatic chain lengths exhibited glass transitions on cooling, but as the relative chain lengths were increased, the glass transition temperature rose, but was then replaced by a crystalline state. This behaviour can be rationalised by examining the balance of the number of aliphatic methylene groups relative to the number of hydroxyl groups free to intermolecular hydrogen bond. When the methylene chain is short, the materials behave as classical sugars (i.e., they melt from the solid and then form glassy states upon cooling). With the increase in the aliphatic chain length, the hydrocarbon chain begins to dominate the melting and re-crystallisation processes. In addition, for the materials that have very short alkyl chains (**I–IVa**) and are not liquid-crystalline, as the alkyl chain is increased in length there becomes a balance in the hydrophobic and hydrophilic parts; further increases in the alkyl chain length lead to domination of the hydrophobic parts accompanied by the formation of liquid crystallinity. The melting points were recorded by DSC and represent the melting behaviour of the materials from their crystalline states formed by solution crystallisation. The DSC traces are included in the Supporting Information. Once the crystal lattice has collapsed at the melting point, only glassification occurs on subsequent cooling for the short-chain homologues, whereas the long-chain homologues re-crystallise. For the materials in which the smectic phases are injected into the homologous series and the melting points are close to room temperature, it should be noted that the sample might be in a state in which there is a mixture of crystal forms and glassy states due to difficulties in crystallisation of the materials from solution; hence the enthalpy values can appear unusually low.

The increase in the clearing point across each series of compounds can be directly related to the hydrophobic–hydrophilic balance, which has previously been demonstrated

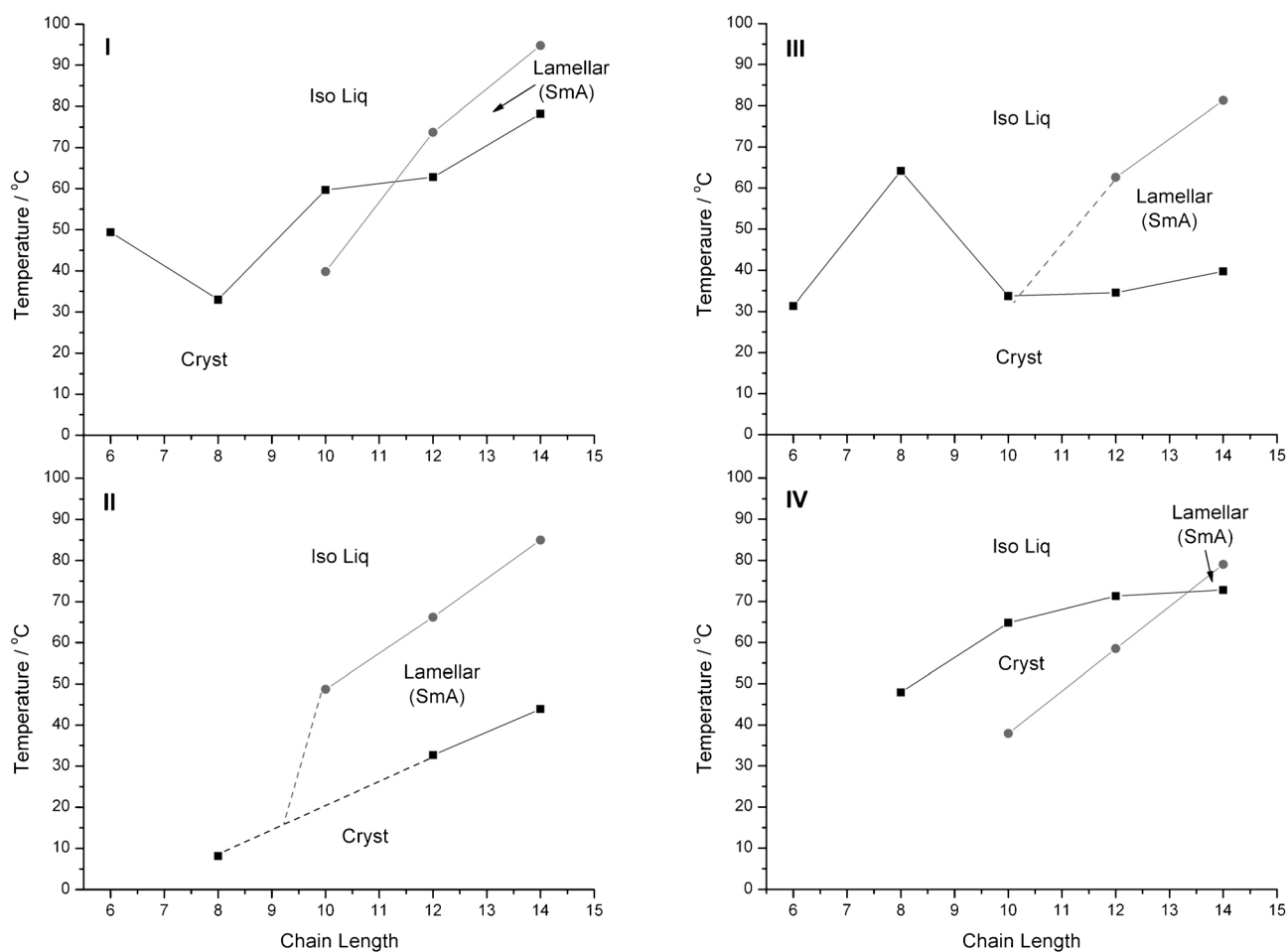


Figure 4. Transition temperature [°C] as a function of chain length ( $n$ ) for **Ia-e**, **Ila-e**, **IIla-e** and **IVa-e**.

in alkyl  $\beta$ -D-glucosides.<sup>[25–27]</sup> Figure 4 shows the transition temperatures for the homologous series **I–IV** as a function of the aliphatic chain length. In each case the clearing point is shown to increase linearly with respect to the increase in chain length. This behaviour indicates that the different transition temperatures between the series of compounds must either be related to the position of substitution of the aliphatic chain on the sugar unit or to the extent of the intramolecular hydrogen bonding that is possible between the hydroxyl group associated with the alkyl chain and the hydroxyl groups in the sugar unit. In this series of compounds, varying the substitution position of the alkyl chain around the glucoside has little effect on the clearing point (79–94°C), relative to the melting points of the compounds. Lower melting points are observed for the compounds substituted at O3 and O4 (**II** and **III**) and higher melting points for the compounds substituted at O2 and O6 (**I** and **IV**). This behaviour is similar to that observed for a series of *O*-dodecyl pyranoses, whereby a change in the substitution position of the dodecyl chain has little effect on the clearing point, but conversely the substitution at O2 and O6 results

in much lower melting points than for the O3 and O4 substitution.<sup>[22]</sup>

It has been clearly demonstrated that the increase in the mesomorphic behaviour of this series of compounds is related to the length of the aliphatic chain attached to the glucoside unit, but the position of attachment also affects the stability of the mesophase formation. Figure 5 shows the isotropisation temperature for the C10–14 homologues (**I–IVc-e**) as a function of substitution position on the sugar unit.

The longer chain lengths (C12 and C14) exhibit consistent behaviour whereby the isotropisation temperature decrease  $O2 > O3 > O4 > O6$  and whereby the number of methylene units in the chain is high enough to dilute the effects of the inter- and intramolecular hydrogen bonding of the hydroxyl groups. However, this behaviour is not observed for the C10 series. This series is on the limit at which there is a strong dependence on the intramolecular and intermolecular hydrogen bonding, which is critically affected by the position of attachment of the chain to the sugar. In this series, the O2 (**Ic**) substitution has a lower clearing point than the O3 (**IIc**), whereas the O4 (**IIIc**) is no longer liquid-crystalline, and the O6 (**IVc**) is similar to O2. This observation indi-

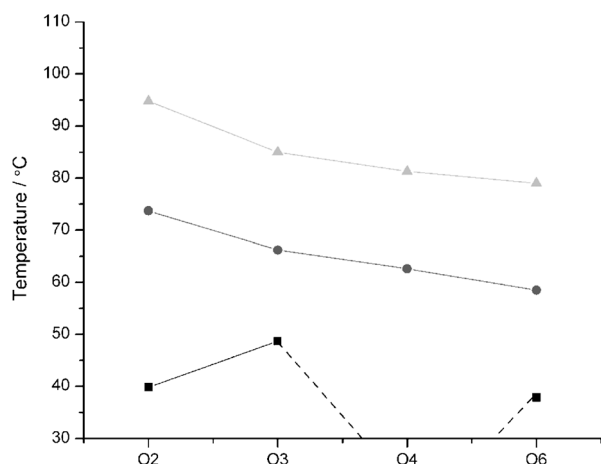


Figure 5. Smectic A to isotropic liquid transition temperature [°C] as a function of substitution position O2 (**Ic–e**), O3 (**IIc–e**), O4 (**IIIc–e**) and O6 (**IVc–e**). ■ = c; ● = d; ▲ = e.

icates that there are probably some intramolecular species that are present in the O3 or O4 materials that could either enhance the liquid-crystalline behaviour, as in the case of O3 (**IIc**), or suppress it, as in the case of O4 (**IVc**).

In order to comprehend the effects of introducing an additional hydroxyl group into the alkyl chains of the substituted glucosides, a comparison between the **IV** series and the previously reported compound **9a** was drawn. Compound **9a** exhibits a smectic A phase, whereas the analogue **IVa** does not exhibit mesomorphism. This comparison shows that at short alkyl chain length the hydrophobic–hydrophilic balance is critical to mesophase formation (i.e., the ratio of the number of OH groups relative to a constant aliphatic chain length dominates). However, for longer aliphatic chain lengths, the relative proportion of the OH content is less, and so the comparative materials have similar clearing points.

In order to investigate the possible intramolecular hydrogen-bonding interactions in the homologous series, energy-minimised models of both enantiomers of compounds **Ia**, **IIa**, **IIIa** and **IVa** were examined in the gas phase at absolute zero (on the basis of energy minimisations in ChemDraw 3D using MM2 and MMFF94 force fields), as shown in Figure 6. There was not a significant difference in the structure or the distance of the hydrogen bonding for each of the enantiomers and therefore the discussion can be applied to either stereoisomer. The distance between each of the neighbouring hydroxyl groups of the glucoside to the hydroxyl group located in the alkyl chain was measured; the closest interaction distances are shown in the models. Compounds **Ia** and **IVa** only have the possibility of hydrogen bonding to one neighbour, whereas compounds **IIa** and **IIIa** have the possibility to hydrogen bond to one of two neighbours (only one of the two orientations for **IIa** and **IIIa** is shown in Figure 6, for which the effective hydrogen-bonding distance is 3.9–4.0 Å). In these configurations the structure is more rigid through the intramolecular hydrogen bonding

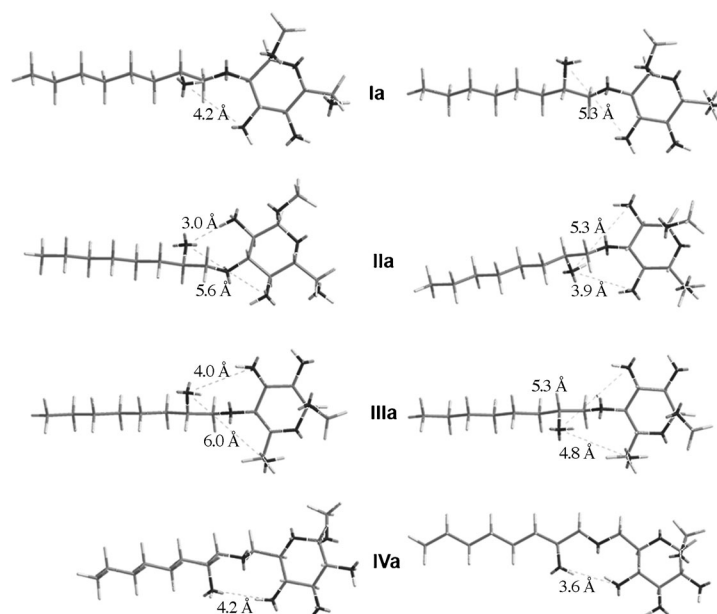


Figure 6. Energy-minimised models of **Ia**, **IIa**, **IIIa** and **IVa**.

in which the alkyl chain and glucoside unit are fixed in position with respect to each other. In order to rationalise whether there is intramolecular or intermolecular hydrogen bonding, it is important to examine the enthalpies of the smectic A to isotropic liquid transition. Table 6 shows the

Table 6. Enthalpies ( $\Delta H$ ) and entropies ( $\Delta S$ ) for smectic A to isotropic liquid transitions for compounds showing liquid-crystalline mesophases.

Compound	$\Delta H$ [J mol <sup>-1</sup> ]	$T$ [K]	$\Delta S$ [J mol <sup>-1</sup> K <sup>-1</sup> ]	$\Delta S/R$ <sup>[a]</sup>
<b>Ic</b>	618	312.8	1.98	0.24
<b>Id</b>	764	346.7	2.20	0.27
<b>Ie</b>	1011	367.8	2.75	0.33
<b>IIc</b>	1344	321.7	4.18	0.50
<b>IIe</b>	2297	339.2	6.77	0.81
<b>IIIc</b>	1075	358	3.00	0.36
<b>IIIe</b>	116	335.6	0.35	0.04
<b>IVc</b>	790	310.9	2.54	0.31
<b>IVe</b>	940	331.5	2.84	0.34
<b>IVe</b>	732	352.0	2.08	0.25

[a]  $R$  is the universal gas constant (8.314472 J K<sup>-1</sup> mol<sup>-1</sup>).

relative enthalpies for all the homologues and their respective normalised entropies. In general the enthalpy of the transition increases as the chain length increases, which indicates that the mesophase is becoming more organised and less like the liquid as the chain length is increased. Typical values of 0.7–0.9 kJ mol<sup>-1</sup> are observed. Interestingly, compounds in series **III** have lower enthalpies of transition and very low  $S/R$  values, which means that these molecules are more disorganised, and explains why the smectic A phase is not observed for the C10 homologue. This result also indicates that it is probable that the hydroxyl groups around the sugar head group are intramolecularly hydrogen bonding, which reduces the propensity of the material to organise

into a lamellar structure that is stabilised by intermolecular hydrogen bonding. Conversely, compounds substituted in the O3 position, series **II**, all exhibit large enthalpies for the clearing-point transition, and *S/R* values are higher than any of the other homologues, which suggests that the materials self-organise more easily into lamellar structures, and this indicates enhanced intermolecular hydrogen bonding. The enthalpies and entropies of the clearing transitions show that the series with O4 substitution must have a relatively reduced hydrophobic–hydrophilic balance, which leads to a reduction in the mesophase stability. The modelling indicates that it is possible for intramolecular hydrogen bonding to occur between the hydroxyl group of the aliphatic chain and the O4 hydroxyl unit of the sugar head group. Such interactions lead to the formation of a pseudo-six-membered ring, thereby increasing the size of the head group relative to the tail. This shift in the balance of the head/tail ratio leads to a reduction in the observed mesomorphic stability. However, as the alkyl chain is extended, its flexibility is expected to interfere in this process.

The melting behaviour can also be considered as a function of intermolecular hydrogen bonding. Compounds of series **I** and **IV** have all the hydroxyl groups on one side of the head group plus chain, whereby the alkyl chain can be oriented so as not to interfere with the head-group interactions, and the effective number of hydroxyl groups available for intermolecular hydrogen bonding is not significantly different to the previously reported alkylglucosides. However, compounds of series **II** and **III** have the alkyl chain splitting the hydroxyl environment whereby the chain can sterically interfere with the head-group interactions. Additionally, one could argue that the extent of the intermolecular hydrogen bonding is partially decreased due to the number of free hydroxyl groups being reduced through two of these groups dynamically interacting with the hydroxyl unit of the alkyl chain. Hence the melting points for these series of compounds are much lower than for compounds of series **I** and **IV**. Compounds of series **II** would give a mixture of primary and secondary alcohols either side of the molecule, whereas compounds of series **III** would only leave one side with two secondary alcohols and one side with a single primary alcohol.

**Lyotropic behaviour:** The concentration-dependent lyotropic behaviour of the materials (**Ib–e** to **IVb–e**) was investigated by examining contact preparations, whereby the glu-

Table 7. Lyotropic behaviour of compounds **Ib–e** to **IVb–e**.

	<b>I</b>	<b>II</b>	<b>III</b>	<b>IV</b>
<b>b</b>	cubic hexagonal	lamellar cubic hexagonal	cubic hexagonal	lamellar cubic hexagonal
<b>c</b>	cubic hexagonal	lamellar cubic	lamellar cubic hexagonal	lamellar cubic hexagonal
<b>d</b>	cubic	lamellar cubic	lamellar cubic	lamellar cubic
<b>e</b>	insoluble	insoluble	insoluble	insoluble

coside forms a gradient of concentration with water. The results are summarised in Table 7 and are similar to those previously reported for the alkyl  $\beta$ -D-glucopyranosides.<sup>[28–30]</sup>

The lyotropic behaviour clearly demonstrates that the curvature in the system, due to increasing interactions between the water and the sugar head groups, increases with increasing water content, thus leading to lamellar, cubic and hexagonal phases being formed. At short alkyl chain length (C8–C10) the relative cross-sectional area of the sugar head group compared to the alkyl chain is large and this allows the curvature of the system to be sufficient for cubic and hexagonal phases to be formed as the sugar head group swells. Figure 7 shows the lyotropic lamellar, cubic and hex-

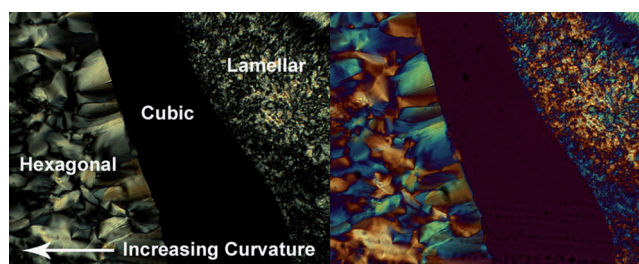


Figure 7. The lyotropic behaviour of compound **IIIc**; left image is between cross polars and right image is viewed with a  $\lambda$  waveplate (100 $\times$  magnification).

agonal phases for compound **IIIc**. At longer chain length (C12), the extra number of methylene units affects the relative cross-sectional area of the sugar group with respect to the chain, and subsequently the curvature of the system is reduced, thus leading to the absence of the cubic phase.

Figure 8 shows the lamellar and cubic phase of compound **III d** in which the Becke line between the cubic phase and the isotropic liquid is clearly visible. The increasing aliphatic

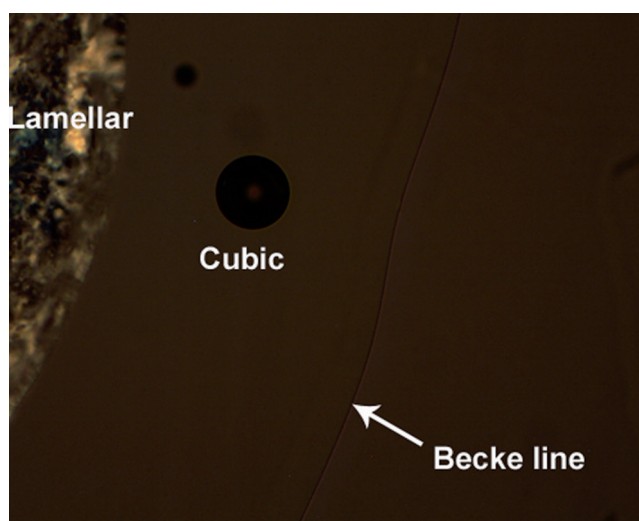


Figure 8. Lamellar and cubic phase of compound **III d** (100 $\times$  magnification).

chain content leads to a reduction in solubility and this is clearly evident in the C14 chain-length homologues, in which the compounds are insoluble in water at room temperature, and still only sparingly soluble at 70°C. In this case, the material crystallised before lyotropic behaviour could be observed.

Interestingly, compounds in which the alkyl chain is attached in the O2 position (series **I**) exhibited increased curvature relative to the other compounds. This indicates that the cross-sectional area of the sugar is larger for these materials than the other homologous series. Series **II** showed a tendency for lower curvature than the other analogues, in which the hexagonal phase was only observed for the shortest chain lengths, which was lost once the chain length reached C10.

## Conclusion

For the four series of glucopyranosides, the clearing points increase linearly with the number of methylene units in the alkyl chain length. If we assume that materials have dichotomous molecular structures composed of polar and non-polar segments (hydrogen bonding to non-hydrogen-bonding), then in comparison with the dodecyl-substituted acyclic polyols,<sup>[1]</sup> we find that there is a delicate balance between the two segments, which supports mesophase formation. Moreover, it appears that the degree of flexibility of the hydrogen-bonding segment (cyclic or alicyclic) is not important in determining mesophase behaviour.

For each addition of a methylene unit, the balance shifts by the same amount, and so too does the clearing point. Hence the clearing points increase incrementally with methylene chain length. Moreover, as the chain gets longer, the clearing points increase, thus indicating a dilution effect of the polar hydrogen-bonding interactions by the alkyl chains, which stabilises lamellar mesophase formation up to the point at which the balance is disturbed as the structure becomes dominated by the fatty chains. This effect is similar to the effects of changing concentration of the liquid component in lyotropic liquid crystals, which begs the question: Do the aliphatic chains act as the solvent for the polar head groups in thermotropic liquid crystals? If this is the case, then thermotropic liquid crystals are, in effect, special cases of inverted lyotropics. As a consequence, glycolipids that possess more than one aliphatic chain exhibit columnar and cubic phases as the proportion of fat in the system is increased due to curvature in the packing together of the molecules.

If we consider the various balances in the architectures of amphitropic liquid crystals (i.e., rigid/flexible, polar/non-polar, polarisable/non-polarisable, aromatic/aliphatic and so on), then for a self-organising thermotropic system, the phase stability will be a summation of all of the balances in structure and properties. In the case of the glycolipids studied here, there is effectively one dominant balance, but for many other systems the overall balance will be complex.

Thus, the hydrophobic–hydrophilic balance and the “hydrophobic effect” are special manifestations of the molecular dichotomy of the structure, whereas for conventional thermotropic liquid crystals the multiple balances will be associated with polychotomy in the structure.

Other descriptors for the formation of self-organised systems have been introduced to the field over the last ten years. These included microphase segregation, nanosegregation, self-sorting and so on; however, these too are manifestations of molecular polychotomy, which inevitably involves complexity of structure. However, increasing complexity does not necessarily mean complexity in topology or interactions; for example, globular supermolecular systems have lower complexities than their linear analogues. In terms of biological systems, primary structures are more complex than quaternary structures.<sup>[31]</sup>

## Acknowledgements

This work has been accomplished under IFCPAR-CEFIPRA (project no. 3805-1) with a post-doctoral grant to M.K.S and research grants and travel grants to A.K. and Y.Q., which are gratefully acknowledged. The authors also thank MENRES and CNRS for financial support and the Chinese Scholarship Council for a fellowship to R.X. Dr M. K. Singh's current address is Aditya Birla Science and Technology Company Ltd, Plot No.1 & 1-A/1, MIDC Taloja, Tal. Panvel, Dist. Raigad 410208 (India).

- [1] J. W. Goodby, V. Görtz, S. J. Cowling, G. Mackenzie, P. Martin, D. Plusquellec, T. Benvegnu, P. Boullanger, D. Lafont, Y. Queneau, S. Chambert, J. Fitremann, *Chem. Soc. Rev.* **2007**, *36*, 1971–2032.
- [2] D. Chandler, *Nature* **2005**, *437*, 640–647.
- [3] J. N. Israelachvili, D. J. Mitchell, B. W. Ninham, *J. Chem. Soc. Faraday Trans. 2* **1976**, *72*, 1525–1568.
- [4] J. N. Israelachvili, S. Marcelja, R. G. Horn, *Q. Rev. Biophys.* **1980**, *13*, 121–200.
- [5] J. N. Israelachvili, *Intermolecular and Surface Forces*, Academic Press, New York, **1985**, pp. 229–271.
- [6] C. Tanford, *The Hydrophobic Effect: Formation of Micelles and Biological Membranes*, Wiley, New York, **1980**, pp. 43–59.
- [7] S. Carnie, J. N. Israelachvili, B. A. Pailthorpe, *Biochim. Biophys. Acta Biomembr.* **1979**, *554*, 340–357.
- [8] R. Nagarajan, *Langmuir* **2002**, *18*, 31–38.
- [9] N. A. Bongartz, J. W. Goodby, *Chem. Commun.* **2010**, *46*, 6452–6454.
- [10] V. Molinier, P. H. Kouwer, J. Fitremann, A. Bouchu, G. Mackenzie, Y. Queneau, J. W. Goodby, *Chem. Eur. J.* **2006**, *12*, 3547–3557.
- [11] V. Molinier, P. H. Kouwer, J. Fitremann, A. Bouchu, G. Mackenzie, Y. Queneau, J. W. Goodby, *Chem. Eur. J.* **2007**, *13*, 1763–1775.
- [12] Y. Queneau, J. Gagnaire, J. J. West, G. Mackenzie, J. W. Goodby, *J. Mater. Chem.* **2001**, *11*, 2839–2844.
- [13] J. W. Goodby, M. J. Watson, G. Mackenzie, S. M. Kelly, S. Bachir, P. Bault, P. Godé, G. Goethals, P. Martin, G. Ronco, P. Villa, *Liq. Cryst.* **1998**, *25*, 139–147.
- [14] A. G. M. Barrett, R. W. Read, D. H. R. Barton, *J. Chem. Soc. Perkin Trans. 1* **1980**, *10*, 2184–2190.
- [15] J. Xue, J. Wu, Z. Guo, *Org. Lett.* **2004**, *6*, 1365–1368.
- [16] P. V. Murphy, J. L. O'Brien, L. J. Gorey-Feret, A. B. Smith, *Tetrahedron* **2003**, *59*, 2259–2271.
- [17] J. Fitremann-Gagnaire, G. Toraman, G. Descotes, A. Bouchu, Y. Queneau, *Tetrahedron Lett.* **1999**, *40*, 2757–2760.
- [18] J. Gagnaire, A. Cornet, A. Bouchu, G. Descotes, Y. Queneau, *Colloids Surf. A* **2000**, *172*, 125–138.

- [19] M. Danel, J. Gagnaire, Y. Queneau, *J. Mol. Catal. A: Chem.* **2002**, *184*, 131–138.
- [20] R. Pierre, I. Adam, J. Fitremann, F. Jerome, A. Bouchu, G. Courtois, J. Barrault, Y. Queneau, *C. R. Chim.* **2004**, *7*, 151–160.
- [21] T. Nobuo, O. Izumi, Y. Shigeki, N. Junzo, *Carbohydr. Res.* **2008**, *343*, 2675–2679.
- [22] R. Miethchen, J. Holz, H. Prade, A. Liptak, *Tetrahedron* **1992**, *48*, 3061–3068.
- [23] A. Smith, P. Nobmann, G. Henehan, P. Bourke, J. Dunne, *Carbohydr. Res.* **2008**, *343*, 2557–2566.
- [24] C. Bayle, A. Gadelle, *Tetrahedron Lett.* **1994**, *35*, 2335–2336.
- [25] H. Prade, R. Miethchen, V. Vill, *J. Prakt. Chem.* **1995**, *337*, 427–440.
- [26] E. Barrall, B. Grant, M. Oxsen, E. T. Samulski, P. C. Moews, J. R. Knox, R. R. Gaskill, J. L. Haberfeld, *Org. Coat. Plast. Chem.* **1979**, *40*, 67–74.
- [27] V. Vill, T. Bocker, J. Thiem, F. Fischer, *Liq. Cryst.* **1989**, *6*, 349–356.
- [28] D. C. Carter, J. R. Ruble, G. A. Jeffrey, *Carbohydr. Res.* **1982**, *102*, 59.
- [29] G. A. Jeffrey, S. Bhattacharjee, *Carbohydr. Res.* **1983**, *115*, 53–58.
- [30] D. L. Dorset, J. P. Rosenbusch, *Chem. Phys. Lipids* **1981**, *29*, 299–307.
- [31] J. W. Goodby, I. M. Saez, S. J. Cowling, J. S. Gasowska, R. A. MacDonald, S. Sia, P. Watson, K. J. Toyne, M. Hird, R. A. Lewis, S.-E. Lee, V. Vaschenko, *Liq. Cryst.* **2009**, *36*, 567–605.

Received: August 16, 2012

Revised: January 9, 2013

Published online: February 20, 2013